

2013-24-0074
Published 09/08/2013

doi:10.4271/2013-24-0074
saealtpow.saejournals.org

# Adaptive Energy Management Strategy Calibration in PHEVs Based on a Sensitivity Study

Federica Lacandia
University of Salento

Laura Tribioli
University of Tuscia

Simona Onori and Giorgio Rizzoni
Center for Automotive Research, OSU

**ABSTRACT**

This paper presents a sensitivity analysis-based study aimed at robustly calibrating the parameters of an adaptive energy management strategy designed for a Plugin Hybrid Electric Vehicle (PHEV). The supervisory control is developed from the Pontryagin's Minimum Principle (PMP) approach and applied to a model of a GM Chevrolet Volt vehicle. The proposed controller aims at minimizing the fuel consumption of the vehicle over a given driving mission, by achieving a blended discharge strategy over the entire cycle. The calibration study is conducted over a wide set of driving conditions and it generates a look-up table and two constant values for the three controller parameters to be used in the in-vehicle implementation. Finally, the calibrated adaptive control strategy is validated against real driving cycles showing the effectiveness of the calibration approach.

**CITATION:** Lacandia, F., Tribioli, L., Onori, S., and Rizzoni, G., "Adaptive Energy Management Strategy Calibration in PHEVs Based on a Sensitivity Study," *SAE Int. J. Alt. Power.* 2(3):2013, doi:10.4271/2013-24-0074.

## INTRODUCTION

The automotive industry is striving to reduce fuel consumption and emissions by improving the efficiency of powertrains and adopting new technologies towards the vehicle electrification. In this scenario, Plug-in Hybird Electric Vehicles (PHEVs) are seen as a promising technology that will have a major impact to reduce fuel usage in the next several decades, [1]. PHEVs represent a compromise between Hybrid Electric Vehicles (HEVs) and Electric Vehicles (EVs), combining benefits of the two architectures. Similarly to a charge-sustaining hybrid vehicle, a PHEV is powered by two energy sources, gasoline and stored electric charge. PHEVs have significantly greater battery capacity than HEVs, and are characterized by the ability of charging the battery from an external source such as the electric power grid, solar power, etc. This external charging ability allows the battery to be depleted during vehicle operation and to be charged when the vehicle is parked, providing the opportunity of using electrical energy in lieu of gasoline, and therefore displacing petroleum consumption, [2]. In a HEV, the battery is charged using the internal combustion engine (ICE) and regenerative braking, and the state of charge (SOC) is maintained in a relatively narrow range throughout the driving cycle, with the general objective of sustaining the battery SOC over a sufficiently long time horizon (for example, a trip), [3]. HEVs can achieve significant improvement in fuel economy by optimizing the power split between the battery and the ICE. The subject of optimal energy management of HEVs has been amply covered in literature, and is reasonably well understood, [4], [5], [6], [7], [8], [9], [10].

Energy management algorithms for PHEVs present additional challenges and opportunities: the fact that the battery is allowed to deplete its charge, and therefore is expected to operate over a much wider range of SOC, requires suitable attention to be paid to how the battery energy is utilized throughout the driving trip, [11], [12]. For example, one strategy might discharge the battery gradually

throughout the driving cycle (blended mode), while another strategy might discharge the battery completely, operating the vehicle in EV-only mode as long as possible, and then operate in charge sustaining operation. The SOC profile used by the control strategy during a trip has been shown to significantly affect the fuel economy of the vehicle in [13], [14], and [15].

This paper presents a solution to the optimal energy management of a PHEV that makes use of well-known principles in optimal control. The problem is solved by applying the Pontryagin's Minimum Principle, suitably modified to yield an adaptive strategy, hereafter called A-PMP. The adaptation of the control parameter of the PMP, called co-state, is realized by use of the idea proposed in [16], [17] for the HEV application, and further extended to the PHEVs in [18]. The open question left unsolved in [18] is the calibration of the parameters of the adaptation law to achieve robustness against different driving cycles for in-vehicle implementation.

In this paper, the Authors propose a calibration approach based on a sensitivity study carried out over a wide set of driving scenarios. The validation of the calibrated strategy is demonstrated over a real driving cycle. The strategy design and calibration study is done for the GM Chevrolet Volt. The vehicle model used in this study is presented in the next section.

# VEHICLE DESCRIPTION AND MODELING

The GM Chevrolet Volt is a powersplit PHEV equipped with a planetary gear set and three clutches, [19], which connect and disconnect the on-board power sources as appropriate to implement various operating modes. The main components of the vehicle powertrain, depicted in Fig. 1, are:

**1.** MOT, which represents the traction electric machine and is a reverse machine;

**2.** GEN, which is the electric generator and can work in reverse mode, as well;

**3.** ICE, which is the internal combustion engine connected to the generator;

**4.** Planetary Gear Set, with three clutches (C1, C2, C3), whose configuration rules the mode of operation of the powertrain;

**5.** Battery pack (BATT), that provides electric power to MOT and GEN when needed.

Table 1 shows the vehicle main characteristics:

***Table 1. Main characteristics of the vehicle***

| | |
|---|---|
| Curb weight | 1715 kg |
| ICE (SI 1.4l) Rated Power | 63kW@4800rpm |
| MOT Rated Power | 111kW@4300rpm |
| GEN Rated Power | 53 kW@4000rpm |
| BATT Max Power (Discharge) | 110 kW |

According to the different configuration of the clutches, the GM Chevrolet Volt powertrain can work in four modes of operation, [19], [20]:

• One-motor EV ($C1 = 1$, $C2 = 0$, $C3 = 0$)[1]: only MOT drives the wheels, while ICE and GEN are switched off.

• Two-motor EV ($C1 = 0$, $C2 = 1$, $C3 = 0$): GEN is connected to the planetary gear set, hence, both MOT and GEN can supply power to the driveline.

• Range-extender mode ($C1 = 1$, $C2 = 0$, $C3 = 1$): MOT alone propels the wheels and the engine generator unit (GENSET) can supply power to the battery and extra power directly to the electric motor, if needed.

• Power-split mode ($C1 = 0$, $C2 = 1$, $C3 = 1$): All the onboard machines (i.e. MOT, GEN, ICE) are connected to the planetary gear set and can supply power to the driveline.

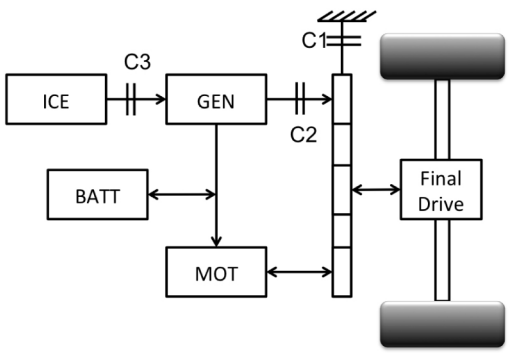


***Figure 1. Chevrolet Volt powertrain and main components.***

The vehicle simulator used in this study and realized in Matlab®/Simulink® environment is an improved version of the tool developed at IFP Energies Nouvelles and provided to all participants of the *PHEV* Control Benchmark competition held during the *IFAC Workshop on Engine and Powertrain Control Simulation and Modeling*, in Rueil-Malmaison, France, in October 2012 (http://www.ecosm12.org). A new battery pack model, described later in this paper, was implemented to replace the simplified one used in the competition. The model used in this study is based on experimental data provided for the LG Chem battery pack used in the GM vehicle, [21].

The forward-looking, energy-based vehicle simulator considers the longitudinal dynamics for the vehicle, the SOC battery dynamics, and employs stationary maps for the electric machines and the internal combustion engine, [19], [22]. The ICE is modeled using its brake specific fuel consumption map, while the electric machines, MOT and GEN, are modeled by means of their efficiency maps.

[1] A value of 1 means that the clutch is closed, a value of 0 means that the clutch is open

## Vehicle Dynamics

The longitudinal vehicle dynamics is dictated by:

$$m\frac{dv_{veh}}{dt} = \frac{T_{pwt} + T_{brake}}{r_{wh}} - mg\sin\alpha - c_0 - c_1 v_{veh} - c_2 v_{veh}^2 \quad (1)$$

where, $m$ is the vehicle mass, $v_{veh}$ the speed of the vehicle, $T_{pwt}$ and $T_{brake}$ are the torques, respectively, at the powertrain and the friction mechanical brakes and $r_{wh}$ is the wheels radius; $g$ is the acceleration of gravity, while the road grade variations (term sinα) represent a loss or a positive contribute, depending on whether the grade is positive or not; $c_0$, $c_1$ and $c_2$ are coefficients, which aim at taking into account the energy losses due to the road load.

## Battery

The battery pack used in the Chevrolet Volt is manufactured by LG Chem and has a configuration of 96S 3P Li-Ion cells, [23]. Table 2 summarizes all the main specifications of the storage system used in the vehicle, [21]:

***Table 2. Battery characteristics***

| | |
|---|---|
| Total energy capacity | 16 kWh |
| Total nominal voltage | 390 V |
| Total peak current | 400 A |
| SOC range | 95%-30% |

The battery model consists of a simple zero-*th* order equivalent circuit model, as shown in Fig 2, where $V_{oc}$ is the open-circuit voltage source, $R_{eq}$ represents the equivalent internal resistance and $V_L$ is the load voltage across the cell terminals. The battery voltage output equation derives from the well-known Kirchhoff voltage law:

$$V_L = V_{oc}(SOC) - I \cdot R_{eq}(SOC) \quad (2)$$

where $I$ is the current across the battery terminals[2]. The battery parameters are a function of both SOC and temperature. In this study, the dependence of the open-circuit voltage on temperature is neglected, on the basis of experimental data, [24]. With regard to the resistance, the investigation is left to future studies and only the dependence with respect to the SOC is considered. The resistance is considered to assume the same values both in charge and discharge, [23].

From Eq. (2), the battery power is a function of SOC and is given by:

$$P_{BATT} = V_L \cdot I = V_{oc}(SOC) \cdot I - I^2 \cdot R_{eq}(SOC) \quad (3)$$

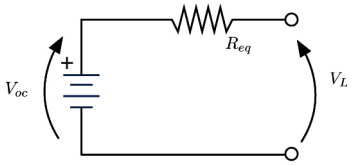


***Figure 2. Zero-th order electrical circuit model of the battery.***

The SOC dynamics is defined as:

$$\dot{SOC} = -\eta_c \cdot \frac{I}{Q_{nom}} \quad (4)$$

where $\eta_c$ represents the coulombic efficiency of the battery, [25], and $Q_{nom}$ is the nominal battery charge capacity. The SOC dynamics can be expressed as a function of the battery power, $P_{BATT}$, by solving Eq. (3) for the current, and replacing it into Eq. (4), to yield:

$$\begin{aligned} \dot{SOC} = & \\ = & -\eta_c \frac{V_{oc}(SOC) - \sqrt{V_{oc}(SOC)^2 - 4 \cdot P_{BATT} \cdot R_{eq}(SOC)}}{2R_{eq}(SOC)Q_{nom}} \\ = & f(SOC(t), P_{BATT}(t)) \end{aligned} \quad (5)$$

where $f(SOC(t);P_{BATT}(t))$ indicates the non linear mapping of the SOC dynamics.

## Planetary Gear Set

In the Chevrolet Volt configuration, the trasmission consists of a planetary gear set, where the motor is connected to the sun, the generator to the ring and the transmission output to the satellite carrier, [20]. In addition, a differential with a fixed gear ratio (final drive in Fig. 1) connects the transmission output to the front wheel axle. The angular speeds of ring ($\omega_r$), sun ($\omega_s$) and carrier ($\omega_c$) are linked by the kinematic Willis relation, [26]:

$$\rho \cdot \omega_r + \omega_s = \omega_c \cdot (\rho + 1) \quad (6)$$

with $\rho$ = 2:24 representing the ratio between the number of teeth of the ring ($N_r$) and the number of teeth of the sun ($N_s$).

The torques relations for the gear set are condensed in the following Eq. (7):

$$\frac{T_r}{\rho} = \frac{T_c}{\rho + 1} = T_s \quad (7)$$

with $T_r$, $T_s$ and $T_c$ being the torques of ring, sun and carrier, respectively, and where:

[2] The current is considered positive in discharge and negative in charge. The same consideration holds for the battery power.

$$\begin{aligned} T_r &= T_{GEN} + C3 \cdot T_{ICE} \\ T_s &= T_{MOT} \\ T_c &= \frac{T_{wh}}{f_d} \end{aligned} \tag{8}$$

with $f_d$ the final drive ratio and $T_{wh}$ the torque at the wheels.

# PROBLEM FORMULATION

The design of the energy management strategy for the GM Chevrolet Volt is cast into a constrained optimization problem aimed at minimizing the fuel consumption over a given driving pattern, while providing the torque demanded by the driver, $T_{wh}$, at each instant of time, satisfying the following constraint:

$$T_{pwt} = T_{wh} \tag{9}$$

Formally, the optimization problem consists on minimizing the following cost function, $J$:

$$J = \int_{t_0}^{t_f} \dot{m}_{fuel}(u(t))\,\mathrm{d}t, \tag{10}$$

where $\dot{m}_{fuel}(u(t))$ is the instantaneous fuel consumption rate, $u(t)$ is the control variable, that is the battery power ($P_{BATT}$), and $[t_f - t_0]$ is the optimization horizon, corresponding to the length of the driving mission. For the sake of fluency the explicit dependence on time is here-after dropped.

The physical limits of the powertrain components are given by

$$\begin{cases} SOC_{min} \leqslant SOC(t) \leqslant SOC_{max} \\ P_{BATT,min} \leqslant P_{BATT}(t) \leqslant P_{BATT,max} \\ T_{MOT,min} \leqslant T_{MOT}(t) \leqslant T_{MOT,max} \\ T_{ICE,min} \leqslant T_{ICE}(t) \leqslant T_{ICE,max} \\ T_{GEN,min} \leqslant T_{GEN}(t) \leqslant T_{GEN,max} \end{cases} \tag{11}$$

where, $SOC_{min}$ and $SOC_{max}$ are the minimum and maximum allowable states of charge, and $P_{BATT,min}$ and $P_{BATT,max}$ are the minimum and maximum thresholds for the battery power. $T_{MOT,min}$ and $T_{MOT,max}$ are the minimum and maximum possible torque values at a given angular velocity for the MOT, and, similarly, $T_{ICE,min}$ and $T_{ICE,max}$, and $T_{GEN,min}$ and $T_{GEN,max}$ are the same physical limits for ICE and GEN, respectively.

In addition to the physical limits of (11), the initial and final conditions of SOC, namely $SOC(t_0)$ and $SOC(t_f)$, must satisfy the following global constraints at $t = t_0$ and $t = t_f$:

$$SOC(t_0) = SOC_0; \quad SOC(t_f) = SOC_f \tag{12}$$

where, in this study, $SOC_0$ is assumed equal to 0.95 indicating that a fully charged battery is available at the beginning of the trip and a $SOC_f$ equal to 0.3 is selected to prevent battery wear at low SOC.

# PONTRYAGIN'S MINIMUM PRINCIPLE

The energy management problem in a PHEV can be solved by using different approaches, including heuristic strategies, numerical optimization methods and optimal control theory, [27]. In this study, the latter approach is used by means of the Pontryagin's Minimum Principle.

The design of the GM Chevrolet Volt, as it is sold commercially today, is that of an Extended Range Electric Vehicle (EREV), that is a vehicle which operates as a pure electric vehicle as long as there is useful energy in the battery, turning into a charge sustaining HEV when the lower SOC threshold is reached. This mode of operation is often referred to as a Charge Depleting/Charge Sustaining strategy (CD-CS). In this paper a different approach is explored which, unlike the CD-CS strategy, provides a blended discharging mode of operation of the powertrain where the final desired value for the SOC, $SOC_f$, is only reached at the end of the driving cycle. The advantages brought by the blended strategy against the CD-CS have already been demonstrated in literature by [15], [28] and in [29], where the PMP was used to minimize a cost function representing the well-to-wheel production of $CO_2$ in a PHEV.

In the formulation of the PMP, the Hamiltonian function, $H$, is defined as follows:

$$H(SOC, u, \lambda) = \dot{m}_{fuel}(u) + \lambda \cdot \dot{SOC}, \tag{13}$$

where $\lambda$ is the co-state and represents the only optimization parameter of the strategy. This equation expresses the contribution of both the energy sources in the vehicle: fuel and electric energy, [7], [30].

The global optimal solution of the problem is found by instantaneously minimizing the Hamiltonian:

$$u^*(t) = arg\ min_u(H(SOC, u, \lambda)) \tag{14}$$

while satisfying the following constraints:

**1.** state variable dynamics and global constraints on SOC:

$$\begin{cases} \dot{SOC}(t) = f(SOC, u) \\ SOC(t_0) = SOC_0 \\ SOC(t_f) = SOC_f \end{cases} \tag{15}$$

**2.** instantaneous constraints on the control and state variables:

$$\begin{cases} u_{min} \leq u \leq u_{max} \\ SOC_{min} \leq SOC \leq SOC_{max} \end{cases} \tag{16}$$

**3.** dynamic evolution of the co-state:

$$\dot{\lambda} = -\frac{\partial H}{\partial SOC} = -\lambda \frac{\partial \dot{SOC}}{\partial SOC}, \tag{17}$$

The PMP is a two boundary condition problem and it is solved using the well-known *shooting method*, [7], [30]. The two boundary conditions are given by Eq. (12). The solution of the PMP results in the optimal SOC, $SOC_{opt}$, and the optimal co-state, $\lambda_{opt}$, trajectories.

In [14] and further in [15], it has been shown that $\lambda_{opt}$ is related to many factors, such as the length of the trip, the features of the driving cycle (grade conditions, speed profile) and the battery characteristics.

Figure 3 shows the SOC profiles, obtained when applying the PMP, as a function of $\lambda_0$, i.e. the initial condition used when integrating Eq. (17). The results were obtained when simulating the vehicle in response to a concatenation of three driving cycles: US06, FHDS, FUDS. A value of $\lambda_0$ greater than the optimal one leads to a final SOC higher than the desired one and, on the other hand, a lower value gives a lower final SOC, making the choice of this parameter a critical step in finding the solution of the optimization problem. The initial value of the co-state which yields to the desired final SOC of 0.3, shown in Fig. 3, is equal to 3.416 *kg*. The high sensitivity of the optimality with respect to the choice of this parameter is a well-known fact when implementing the PMP, [7].

In the PMP problem, the co-state evolves according to Eq. (17). Nevertheless, the variation of this parameter depends on the battery characteristics and in particular on the battery efficiency. The fact that the battery efficiency is almost constant in this application, [21], implies a very small variation of the co-state during the driving mission, as shown in [30] and [31]. The implication of this is that $\lambda(t) = \lambda_0 \ \forall_t \in [t_0, t_f]$ and thus the determination of $\lambda_0 = \lambda_{opt}$ is in what optimality lies.

Figure 3 suggests that the solution of the problem obtained with the PMP results in a quasi-linear trajectory for the SOC, with respect to the traveled distance, as already shown in [13] and [18]. Nonetheless, this is true when there are no variations in the altitude profile, otherwise the SOC trend assumes more of a zigzag-like trajectory, as shown in [15] and [18], and also in the simulation results of Fig. 20 and Fig. 22.

Despite the fact that the optimal solution of the energy management problem using PMP is obtained only via off-line implementation, where an iterative search for $\lambda$ is possible, the non-causal nature of the PMP strategy lends itslef to the design of a causal controller called APMP, where the co-state is adapted as driving conditions change [18].

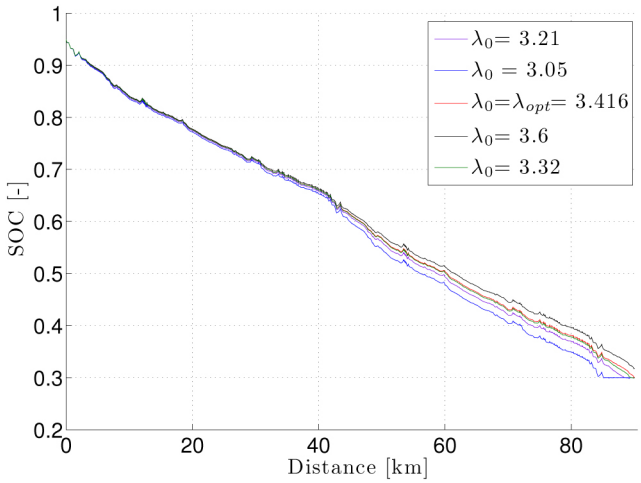


***Figure 3. SOC trajectories w.r.t. distance for variations of $\lambda_0$ for a concatenation of driving cycles (US06, FHDS, FUDS)***

# ADAPTIVE CONTROL STRATEGY

The adaptive control model, A-PMP, is a modification of the one proposed by [17] for HEV applications and already improved by [18] in the case of PHEVs. In particular, the A-PMP is aimed at adapting the co-state as driving conditions change. The co-state is updated in order to "force" the actual SOC to track a linear SOC profile (later referred to as $SOC_{ref}(s)$) with respect to the total traveled distance, that is supposed to be known.

The adaptation is by means of an AutoRegressive Moving Average (ARMA) model, already proposed by [18]:

$$\lambda(s+k) = \frac{\lambda(s)+\lambda(s-k)}{2} + K_p\left[SOC_{ref}(s) - SOC(s)\right] \tag{18}$$

The co-state update is a result of a distance-based adaptation, where a proportional gain is introduced to correct the SOC divergences from the reference curve, $SOC_{ref}(s)$. In Eq. (18), $k$ [km] is the sampling distance, $s$[km] is the current covered distance and $K_p$ [kg] is the proportional gain. $SOC_{ref}(s)$ is defined as an affine function of SOC with respect to the distance, according to the following relation:

$$SOC_{ref}(s) = \alpha + \beta \cdot d \tag{19}$$

where

$$\begin{cases} \alpha = SOC_f \\ \beta = SOC_0 - SOC_f \\ d = \frac{D-s}{D}, \end{cases} \tag{20}$$

where $D$ [km] is the total distance of the trip.

The underlyning fact in the proposed adaptation law is that the desired SOC profile is linear with respect to the distance. This assumption is true only if the road grade is flat. In order to handle more realistic situations (*e.g.* variation of grade) a modification to the adaptation law is proposed, based on [18], as well as some exceptions to the adaptation law (Eq. (18)) are considered and implemented in the controller. In particular:

**1.** when $SOC(s) = SOC_{ref}(s)$, the value of λ is reset and set equal to the initial value $\lambda_0$, to avoid instabilities due to the proportional controller;

**2.** to avoid charging the battery at the initial or final parts of the driving mission, the possibility of using only the electric machines is considered by setting λ equal to zero. As the co-state has the physical meaning of an equivalence factor between fuel and battery usage, [17], a condition of $\lambda = 0$ in Eq. (13) encourages the use of the battery instead of the ICE;

**3.** if $SOC(s) > 0{:}35$ when approaching the end of the trip $\lambda = 0$ is imposed, as in the previous case, to drive only with the electric motors, switching off the ICE.

# CALIBRATION OF THE ADAPTATION LAW

The parameters of the co-state adaptation law (18), which are:

**1.** the initial co-state value: $\lambda_0$,

**2.** the updating sampling distance: $k$,

**3.** the proportional gain: $K_p$

need to be calibrated for (18) to be used in real-time operation.

In order for the controller to ensure robustness against changing in driving conditions, an investigation on the influence of these parameters on the controller performance is performed by means of a sensitivity study. The objective of the calibration is to ensure that the best value of these parameters is chosen so as to guarantee minimum fuel consumed over different driving cycles.

To this aim, the sensitivity analysis conducted in this study was carried over wide set of driving scenarios (including urban, suburban and highway speed profiles). Flat patterns are considered as baseline, since a relationship between the variations in elevation and the SOC trajectory is in general hard to find, [32], and, in this study, no information about the road grade variation is assumed to be available. The only assumption made is that the average cycle speed and the total traveled distance are known.

The sensitivity analysis is conducted over the following driving cycles:

• NEDC: a standardized cycle composed by urban and extra-urban portions, Fig.4;

• Combined: a cycle composed by the concatenation of US06, FHDS and FUDS, Fig.5;

• Composed Artemis: a pattern consisting of a sequence of Urban, Extra-Urban and Highway Artemis, Fig.6;

• Artemis highway: a standardized highway driving cycle, Fig.7.

The specifications of these cycles are summarized in Table 3, where $v_{avg}$ is the average speed of the cycle, $v_{max}$ is the maximum speed, while $D_{ae}$ identifies the total electric range driven from the beginning of the trip to the point at which the ICE is switched on. This distance is commonly known as *All Electric* range, [1], [12], and depends on SOC utilization range. One can note that cycles with lower average speeds present a larger *All Electric* range. Nevertheless, the simulation campaign demonstrated that a direct correlation would be unfair, since this value, which is related to the driver torque request, is, by means of Eq.(1) more dependent on the average acceleration, rather than the average speed. On the other hand, in this study, only the average cycle speed is assumed known, thus this parameter has been considered prima facie evidence of the aggressiveness of the driving cycle.

***Table 3. Driving cycles features.***

| Cycle | $v_{avg}$ $[km/h]$ | $v_{max}$ $[km/h]$ | $D_{ae}$ $[km]$ |
|---|---|---|---|
| NEDC | 33.6 | 120 | 89.7 |
| Combined | 54.5 | 129 | 75.3 |
| Composed Artemis | 61.1 | 150 | 55.5 |
| Artemis highway | 99.5 | 150 | 46.2 |

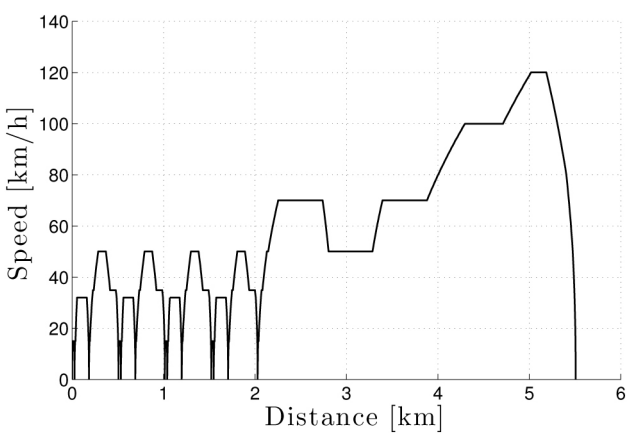


***Figure 4. Speed profile of NEDC driving cycle***

Since the total traveled distance is assumed to be known and the dependence of the optimal solution on this parameter has been shown, [18], different distances were considered in the sensisivity study. The length of the cycles used in the analysis varies between 10 *km* and 500 *km* with a non-constant discretization step, which increases with the distance. In particular, the distance interval of 10-200 *km* is

analized more in depth as it represents a reasonable driving range operated by a PHEV [2].

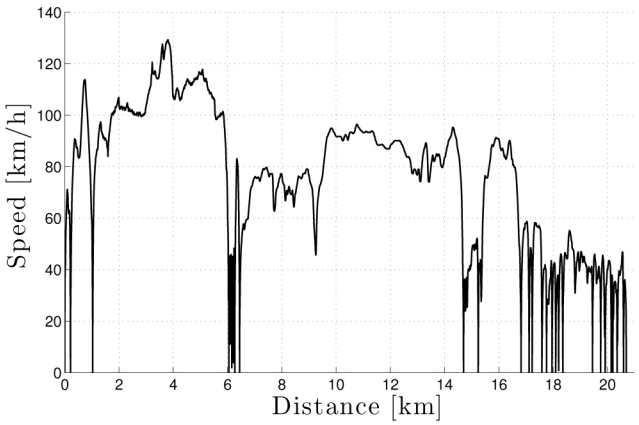


***Figure 5. Speed profile of Combined driving cycle***

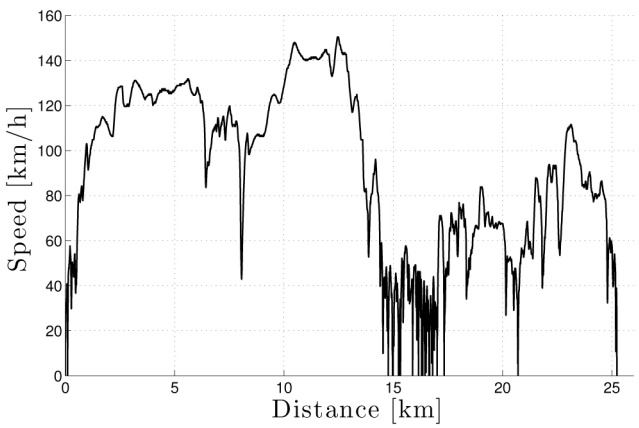


***Figure 6. Speed profile of Composed Artemis driving cycle***

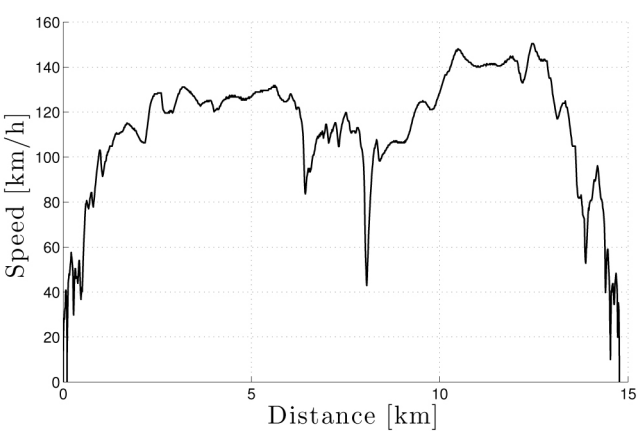


***Figure 7. Speed profile of Artemis highway driving cycle***

## Calibration of the Initial Co-State, $\lambda_0$

The solution of the optimal problem has been already proved to be significantly influenced by this parameter. Being an optimization parameter of the PMP framework, the analysis of the co-state was carried out solving the optimal problem.

The Authors first solve the optimal problem from the PMP for the driving cycles of Table 4, covering distances going from 10 *km* to 500 *km* (see Fig. 8). This information is then coupled with information about the cycle average speed in the 3D map shown in Fig. 9.

It is interesting to notice that the optimal value of $\lambda_0$ is a monotonically increasing function of the total driven distance, as shown in Fig. 8.

As the co-state represents an equivalence factor to convert battery power into an equivalent fuel power, it is easy to see why the optimal value of $\lambda_0$ is equal to zero for distances lower than the *All Electric* range (see Table 3). Forcing $\lambda_0$ to be equal to 0 is what makes the supervisory controller use the battery instead of the engine, in order to meet the global constraint on the final SOC. On the other hand, Fig. 8 also shows that beyond the *All Electric* range, the value of $\lambda_0$ instantly increases to values greater than 3 *kg*. Hence, this value can be recognized as a threshold value, under which the weight of the battery power is not relevant compared to the fuel power and the optimization tool can only choose to use the battery. Figure 8 shows that at great distances the optimal value of $\lambda_0$ reaches an asymptote. This behavior is more pronounced for cycles with high average speeds, while cycles with low average speeds, *e.g.* NEDC, are still characterized by a slight in increase of $\lambda_0$ with the distance. Thus, for high distances, as the weight of the battery power becomes comparable to the fuel power, the vehicle behaves like a pure HEV rather than a PHEV.

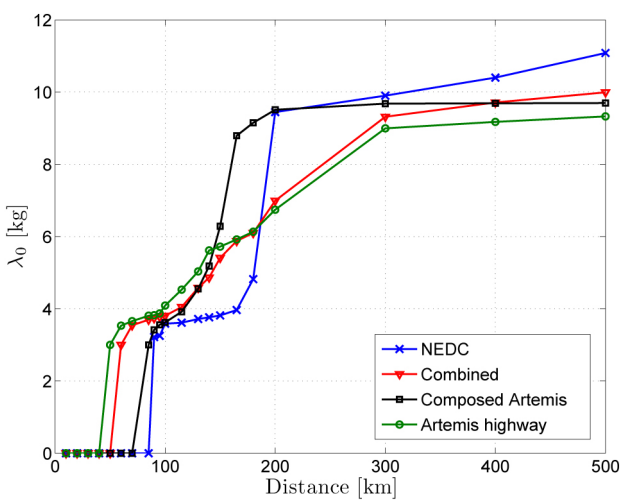


***Figure 8. Trend of λ as a function of distance for different driving cycles***

The final output of this analysis is the map shown in Fig. 9, which is used to initialize $\lambda_0$ as a function of the distance

and the average speed (the only driving information assumed to be known)[3] in the adaptation law of the A-PMP.

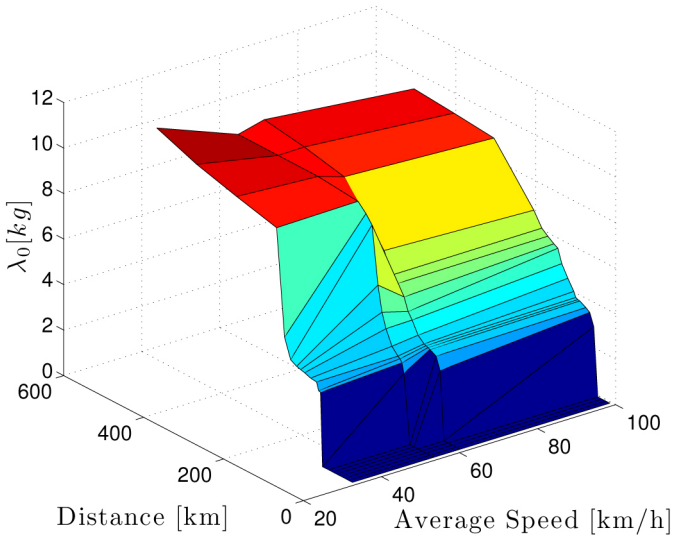


***Figure 9. Map with the values of $\lambda_0$ as a function of distance and average speed***

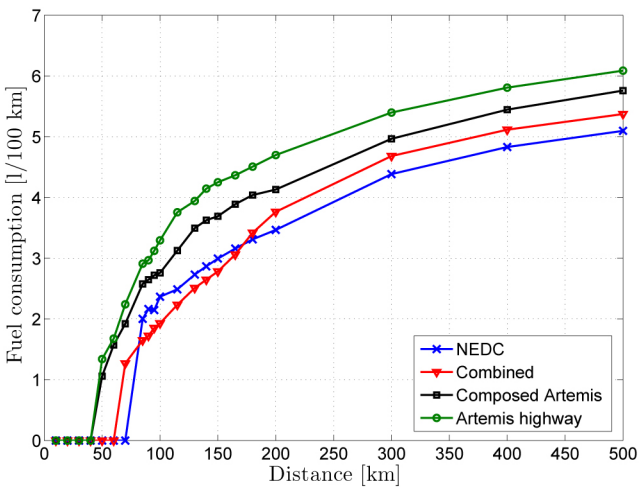


***Figure 10. Optimal fuel consumption as a function of the driving cycle and distance***

Fuel consumption and equivalent fuel consumption are also provided, in Figures 10 and 11 respectively, for the same simulation set. In this paper, the fuel consumption represents the actual amount of fuel consumed during the trip, while the equivalent fuel consumption takes into account also the net amount of battery energy used during the mission. The actual fuel consumed by the engine (see Fig. 10) presents an increasing trend with the trip distance, tending towards an asymptotic value for long distances. On the other hand, the equivalent fuel consumption (see Fig. 11) has an asymmetric trend with respect to the fuel consumption. In fact, for distances lower than the *All Electric* range, only the battery is used as energy source for traction while for greater distances the battery use is discouraged in favor of fuel use. Furthermore, one can note that over large distances both the actual fuel consumption and the equivalent fuel consumption tend to level off, confirming that the powertrain behaves asymptotically like a HEV.

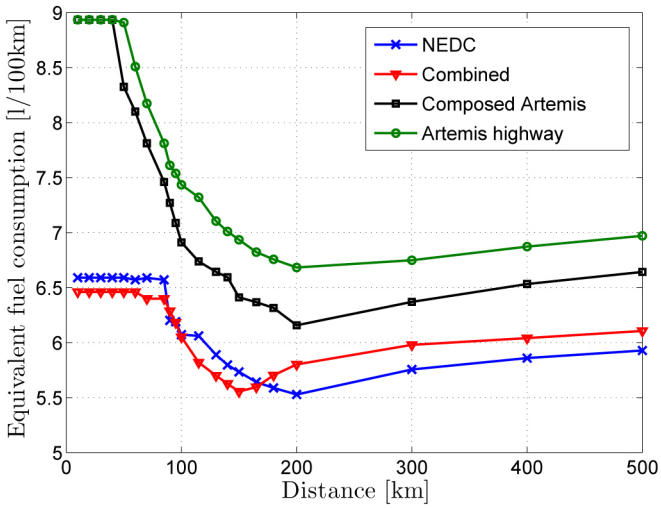


***Figure 11. Equivalent fuel consumption as a function of the driving cycle and distance***

## Calibration of the Sampling Distance, *K*

The sensitivity analysis on this parameter aims at understanding the benefits which can be obtained when increasing or reducing the value of sampling distance $k$ with respect to the fuel consumption. For this analysis, the initialization map, built after the sensitivity study on $\lambda_0$, was implemented in the A-PMP controller. The value of $K_p$ was hold, as a first attempt, equal to 5 *kg*, as in [18].

Results are presented for a driven distance of 120 *km*. Simulations with different distances, i.e. from 0 *km* to 120 *km*, gave similar results, and they are not presented in the paper.

In particular, Fig. 12 shows the fuel consumption as a function of $k$, normalized with respect to the optimal fuel consumption obtained with the PMP-based controller. The fuel consumption is practically insensitive to variations of $k$, for driving cycles with high average speeds, *i.e.* Artemis highway, Composed Artemis and Combined. The percentage variation of fuel consumption for these cycles falls in a very small range, while for the NEDC, characterized by the lowest average speed, the variation of the normalized fuel consumption is slightly more pronounced. This can depend on the fact that the first part of this driving cycle is composed by four UDCs (Urban Driving Cycles), with a length shorter

[3] For driving cycles different from the ones employed in this calibration campaign, i.e. with different grade variations, lengths or average speeds, one can interpolate between the values in the map.

than 2 *km* (see Fig. 4). Values of *k* greater than 2 *km* can thus result in a loss of information about this portion of the cycle, giving worse results.

The worst-case scenario produces an error of 4%, for a *k* of 4 *km*, while for a value of 1 *km* the error is within 2%.

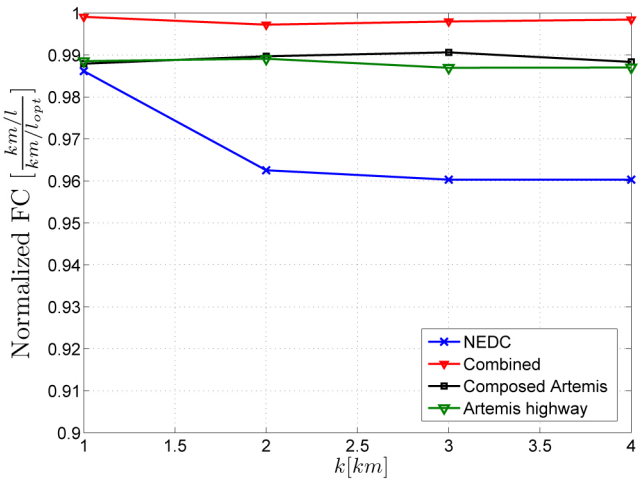


***Figure 12. Normalized fuel consumption variation as a function of k***

## Calibration of the Proportional Gain, $K_P$

The proportional gain in the adaptation law has the role of correcting SOC deviations from the reference signal, $SOC_{ref}$ (*s*). The fuel consumption is analyzed against variations of $K_p$ by setting $k = 1km$.

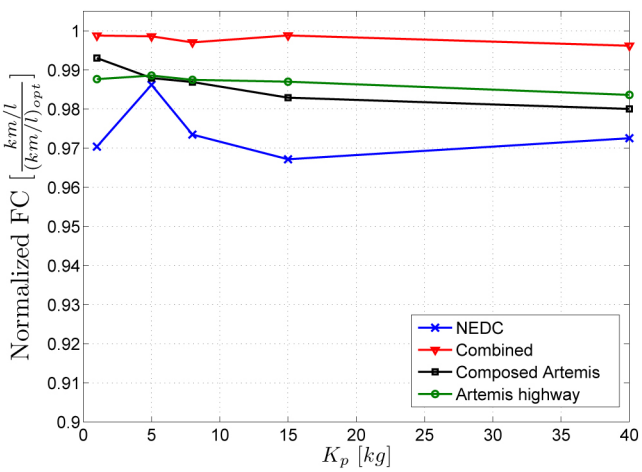


***Figure 13. Normalized fuel consumption variation as a function of $K_p$***

In Fig. 13 the fuel consumption, normalized with respect to the PMP solution, varies as a function of $K_p$. The maximum fuel consumption deviation is of around 3%, while the optimal value of $K_p$ gives the minimum error, *i.e.* 1%. This value, corresponding to 5 *kg* has been chosen for the proportional gain.

It is worth noting that the normalized fuel consumption remains almost constant as $K_p$ varies, the performance of the algorithm not being influenced by the variation of this parameter, as also was the case for *k*. The controller results in being robust with regard to both these parameters.

The outcome of the sensitivity analysis is such that the following values are used to calibrate the A-PMP: $\lambda_0$ (maps), $k = 1km$ and $K_p = 5kg$.

# VALIDATION

In this section, the calibrated adaptive control law is then validated by simulating the vehicle behavior over realistic driving cycles, significantly different from the regulatory driving cycles used for the calibration process.

The first cycle, hereafter called Urban, is shown in Fig.14 and represents a urban cycle of 100 *km*, whose characteristics are listed in Table 4. This cycle was obtained by means of SUMO (Simulation of Urban MObility), which is an open-source traffic simulation package developed since 2000 by the Institute of Transportation Research at the German Aerospace Center. The use of this tool, taking into account driver ability and traffic conditions, generates driving profiles which can allow more realistic estimations of fuel consumption, [33].

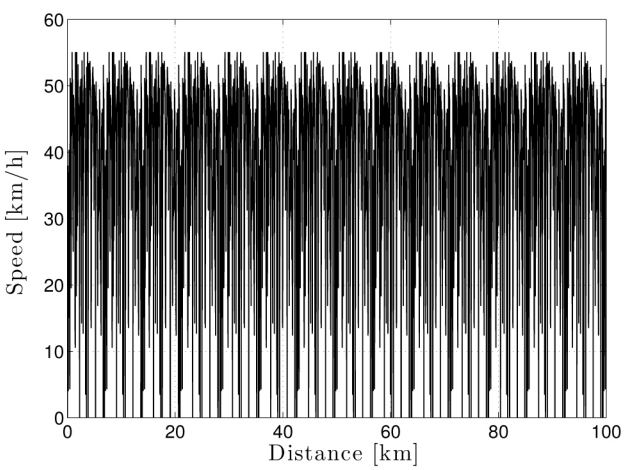


***Figure 14. Speed profile of the Urban Cycle***

The second driving cycle used, later referred to as Extraurban, is shown in Fig.16. This cycle is a result of a GPS acquisition for a total length of 150 *km*. Both flat patterns and road with elevation are considered. Figure 17 shows the grade profile used in combination with the Urban cycle, while Fig.18 portrays the grade profile for the Extraurban cycle.

The features of the driving cycles are summarized in Table 4:

***Table 4. Real cycles features***

| Characteristic | Urban | Extraurban |
|---|---|---|
| Average Speed [km/h] | 29.72 | 50 |
| Maximum Speed [km/h] | 55 | 115.37 |
| Length [km] | 100 | 150 |

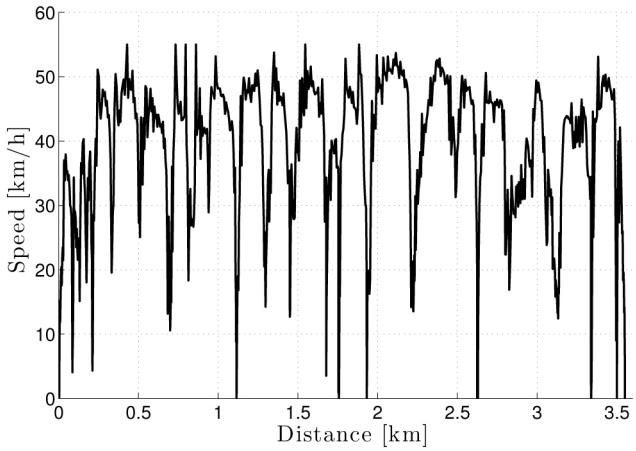


***Figure 15. Elementary cycle of the Urban Cycle, speed profile***

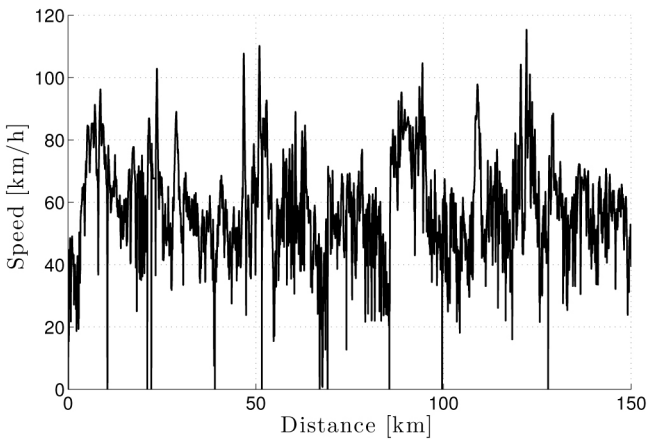


***Figure 16. Speed profile of the Extraurban Cycle***

Figures 19 and 21 show the SOC trajectories for the Urban and Extraurban scenarios (with no grade variations). Both profiles are very close to the reference SOC, $SOC_{ref}$. On the other hand, Figures 20 and 22 show that, in presence of altitude variations, the deviation of SOC from the reference trajectory is highly pronounced and increases with the steepness of the grade profile. The constraint on the final SOC is not met, in neither of the two cases, since both the grade profiles are characterized by a downhill segment in the final part of the trip. In such an event, the battery is charged even if $\lambda$ is set equal to zero, thus switching off the engine. It is worth noting that, if the knowledge of the upcoming elevation profile were available, by means of on-board traffic relevation systems such as cloud computing, GPS (Global Positioning System), ITS (Intelligent Transportation System) or GIS (Geographical Information System), one could in principle think of feeding this information back to the controller to track an optimal non-linear SOC profile, achieving better results. Nonetheless, the possibility of having information about the grade profile is left to future studies.

Table 5 provides a comparison of the A-PMP solution with the optimal solution of the PMP and the results obtained with the CD-CS strategy, currently used on-board of the GM vehicle. The same results are also depicted in Fig. 23. In this work, the CD-CS strategy has been modeled depleting the battery by making the powertrain operate in *One-motor EV* or *Two-motor EV* modes, depending on the power request and then sustaining the SOC by means of an Adaptive-ECMS algorithm, [17], that ensures the SOC to be regulated at the constant value of 0.3 SOC.

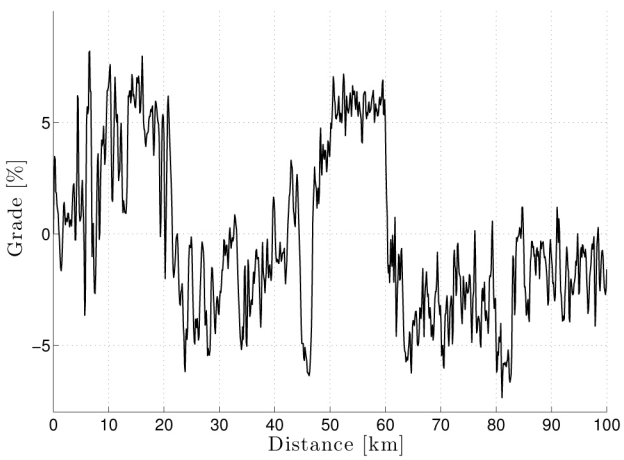


***Figure 17. Grade profile used with the Urban Cycle of Fig. 15***

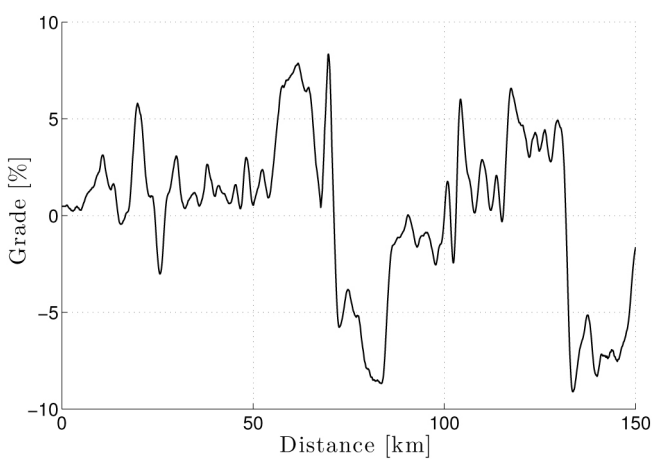


***Figure 18. Grade profile used with the Extraurban Cycle of Fig. 17***

***Table 5. Strategies Comparison***

| Cycle | Strategy | FC [MPG] | Error [%] |
|---|---|---|---|
| Urban no grade | PMP | 81.53 | - |
| Urban no grade | A-PMP | 80.99 | -0.66 |
| Urban no grade | CD-CS | 72.35 | -11.2 |
| Urban grade | PMP | 73.43 | - |
| Urban grade | A-PMP | 68.29 | -6.99 |
| Urban grade | CD-CS | 58.15 | -20.1 |
| Extraurban no grade | PMP | 101.63 | - |
| Extraurban no grade | A-PMP | 100.72 | -0.89 |
| Extraurban no grade | CD-CS | 79.29 | -21.96 |
| Extraurban grade | PMP | 70.79 | - |
| Extraurban grade | A-PMP | 58.13 | -17.88 |
| Extraurban grade | CD-CS | 45.03 | -36.39 |

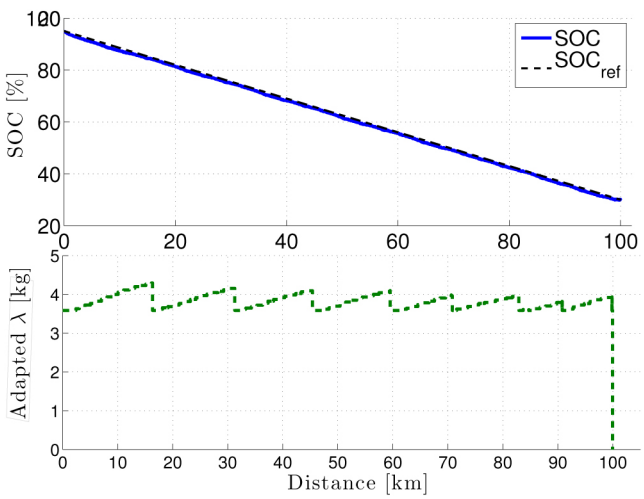


***Figure 19. SOC and adapted λ trajectories for the Urban Cycle without grade, k = 1 km and $K_p$ = 5 kg***

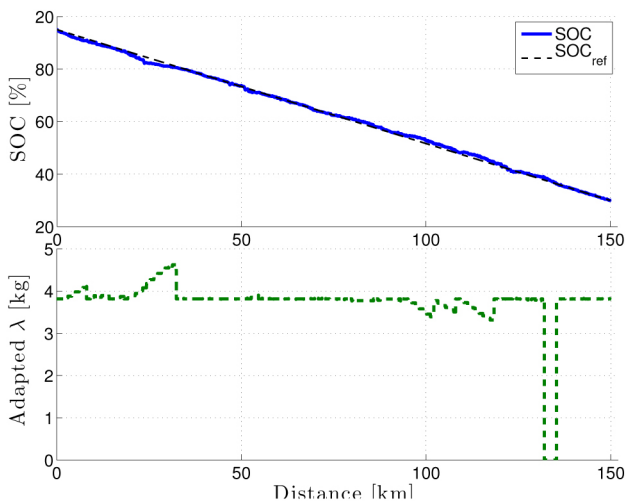


***Figure 21. SOC and adapted λ trajectories for the Extraurban Cycle without grade, k = 1 km and Kp = 5 kg***

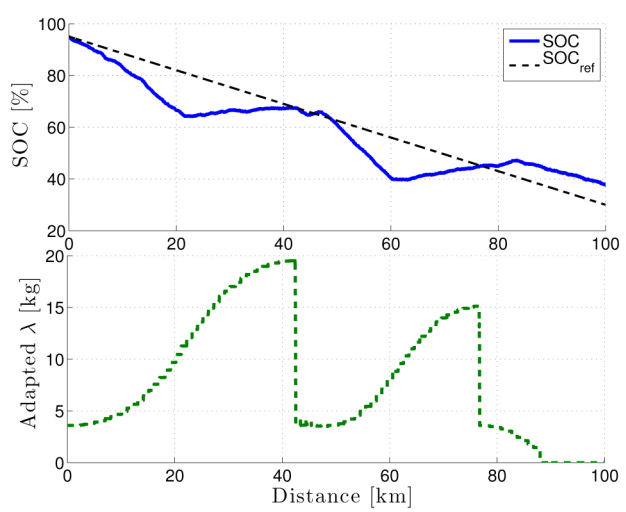


***Figure 20. SOC and adapted λ trajectories for the Urban Cycle with grade, k = 1 km and $K_p$ = 5 kg***

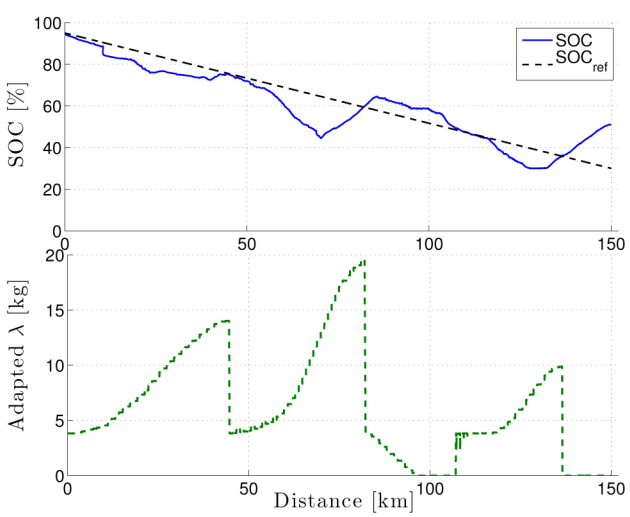


***Figure 22. SOC and adapted λ trajectories for the Extraurban Cycle with grade, k = 1 km and $K_p$ = 5 kg***

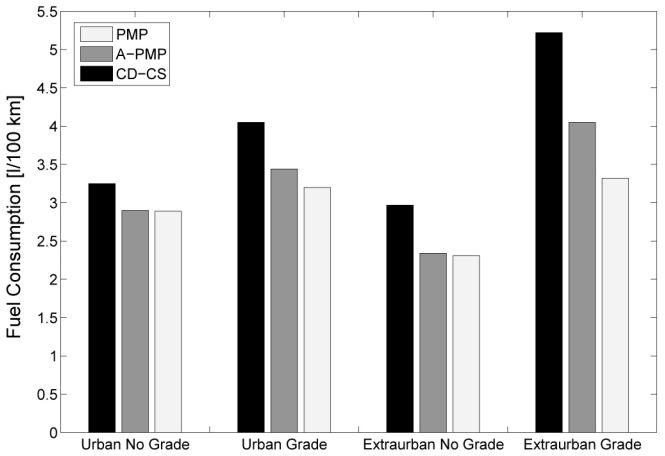


***Figure 23. Comparison of the fuel consumption obtained with the three strategies in the different scenarios***

It can be seen that, in every scenario, the adaptive strategy performs better than the CD-CS strategy, giving results close-to-the-optimum even with aggressive altitude profiles. In particular, the fuel consumption of the A-PMP is always within 1% of the optimal solution from PMP in no grade conditions, and reaches a maximum discrepance of around 20% in the scenarios with variable altitude profiles. On the contrary, with the CD-CS strategy the difference is significant also without grade, with an increase in fuel consumption of at least 11% in no grade conditions and up to 36% when grade is considered.

# CONCLUSIONS

In this paper a sensitivity analysis of an adaptive supervisory controller, based on PMP, for the energy management of PHEVs has been presented. By making only use of the knowledge of total traveled distance and cycle average speed, the algorithm proposed adapts the optimization parameter of the PMP, *i.e*. the co-state, in order to track a reference linear SOC trajectory. This adaptation law introduces some parameters which require to be calibrated.

In particular, two parameters of the adaptation law have been shown to have small influence on the fuel consumption, and such a constant value was selected, irrespective to the driving conditions.

The calibration parameter with the greatest importance has been shown to be the critical value of the co-state. Thorough analysis of this parameter with respect to the length of trip and nature/characteristics of the cycles was conducted that generated a look-up table that the supervisory controller would interrogate during vehicle operation.

Results presented to validate the calibration have shown that an accurate initialization database for the co-state as a function of the driving information, assumed to be known (*i.e*. traveled distance and average speed), allows obtaining results close-to-the-optimum even in driving conditions far from the standardized speed profiles considered in the calibration phase. In particular, realistic driving cycles have been simulated obtaining encouraging results both with and without road grade variations. The A-PMP is shown to perform always better than the CD-CS strategy, presenting in the worst case, only a 20% increase in fuel consumption of the adaptive controller with respect to the PMP, against an increase of 36% obtained by the CD-CS in the same scenario.

# REFERENCES


1. Markel T. and Simpson, A. “Cost Benefit Analysis of Plug-In Hybrid Electric Vehicle Technology,” *WEVA, J.*, vol. 1, 2006.
2. Markel, T. Smith, K. and Pesaran, A. “PHEV energy storage performance/life/cost tradeoff analysis,” *in Proceedings of the 8th Advanced Automotive Battery Conference*, Tampa, FL, 2008.
3. Sciarretta A. and Guzzella, L. “Control of Hybrid Electric Vehicles,” *Control Systems, IEEE*, vol. 27, no. 2, pp. 60-70, 2007.
4. Brahma, A. Guezennec, Y. and Rizzoni, G. “Optimal energy management in series hybrid electric vehicles,” in *Proceedings of the American Control Conference 2000*, vol. 1, no. 6, 2000, pp. 60-64.
5. Paganelli, G. Guerra, T. Delprat, S. Santin, J. Delhom, M. and Combes, E. “Simulation and assestment of power control strategies for a parallel hybrid car,” *Proceedings of the Institution of Mechanical Engineers, Part D: Journal of Automobile Engineering*, vol. 214, no. 7, pp. 705-717, 2000.
6. Lin, C. Kang, J. Grizzle, J. and Peng, H. “Energy management strategy for a parallel hybrid electric truck,” *Proceedings of the American Control Conference*, vol. 4, p. 28782883, 2001.
7. Serrao, L. Onori, S. and Rizzoni, G. “A comparative analysis of energy management strategies for hybrid electric vehicles,” *Dynamic Systems, Measurement and Control*, J., vol. 133, no. 3, p. 031092(9pages), 2011.
8. Serrao L. and Rizzoni, G. “Optimal control of power split for a hybrid electric refuse vehicle,” *in Proceedings of the American Control Conference*, 2008.
9. Kim, N. Cha, S. and Peng, H. “Optimal control of hybrid electric vehicles based on Pontryagin's Minimum Principle,” *Control Systems Technology, IEEE Transactions on.*, vol. 19, no. 5, pp. 1279-1287, 2011.
10. Bianchi, D. Rolando, L. Serrao, L. Onori, S. Rizzoni, G. Al-Khayat N., Hsieh, T. M. and Kang, P. “Layered control strategies for hybrid electric vehicles based on optimal control,” *Electric and Hybrid Vehicles, Int. J.*, vol. 3, no. 2, p. 191217, 2011.
11. Moura S. J., Callaway, D. S. Fathy, H. K. and Stein, J. L. “Tradeoffs between battery energy capacity and stochastic optimal power management in plug-in hybrid electric vehicles,” *Power Sources, J.*, vol. 195, no. 9, pp. 2979-2988, 2009.
12. Tulpule, P. Marano, V. and Rizzoni, G. “Effects of different PHEV Control Strategies on Vehicle Performance,” in *Proceedings of the American Control Conference*, 2009.
13. Marano, V. Tulpule, P. and Rizzoni, G. “Energy Management for Plug-in Hybrid Electric Vehicles using Equivalent Consumption Minimization Strategy,” *Electric and Hybrid Vehicles, Int. J.*, vol. 2, no. 4, pp. 329-350, 2010.
14. Sharma, O. P. Onori, S. and Guezennec, Y. “Analysis of the Pontryagin's Minimum Principle-based Energy Management Strategy for PHEV Applications,” in *Proceedings of the 5th Annual Dynamic Systems and Control Conference and 11th Motion and Vibration Conference*, 2012.
15. Tribioli L. and Onori, S. “Analysis of Energy Management Strategies in Plug-in Hybrid Electric Vehicles: application to the Chevrolet Volt,” in *Proceedings of the American Control Conference*, 2013.
16. Onori S. and Serrao, L. “On Adaptive-ECMS strategies for Hybrid Electric Vehicles,” *Les Recontres Scientifiques d'IFP Energies nouvelles - RHEVE 2011*, 2011.
17. Onori, S. Serrao, L. and Rizzoni, G. “Adaptive Equivalent Consumption Minimization Strategy for HEVs,” in *Proceedings of the ASME Dynamic Systems and Control Conference*, 2010.
18. Sharma, O. P. “A practical implementation of a near optimal energy management strategy based on the Pontryagin's Minimum Principle in a PHEV,” Master's thesis, The Ohio State University, 2012.
19. Grebe U. D. and Nitz, L. T. “VOLTEC - The propulsion system for Chevrolet Volt and Opel Ampera,” *ATZ Autotechnology*, 2011.
20. Miller, M., Holmes, A., Conlon, B., and Savagian, P., “The GM “Voltec” 4ET50 Multi-Mode Electric Transaxle,” *SAE Int. J. Engines* 4(1):1102-1114, 2011, doi:10.4271/2011-01-0887.
21. Parrish, R., Elankumaran, K., Gandhi, M., Nance, B. et al., “Voltec Battery Design and Manufacturing,” SAE Technical Paper 2011-01-1360, 2011, doi:10.4271/2011-01-1360.

**22.** Falieres, Q. Grasset, O. Roblet, K. Xu, Y. Noiret, C. Serrao, L. and Sciarretta, A. "A contradictory analysis of GM Voltec powertrain," in *Proceedings of the European Electric Vehicle Conference*, 2011.

**23.** Alamgir M. and Chung, G. C. "A high-performance PHEV battery pack, Project ID: ES002," *LG Chem Power/LG Chem*, 2012.

**24.** Plett, G. L. "Sigma-point Kalman filtering for battery management systems of LiPo-based HEV battery packs. Part 2: Simultaneous state and parameter estimation," *Power Sources, J.*, vol. 161, no. 2, pp. 1369-1384, 2006.

**25.** Sciaretta A. and Guzzella, L. *Vehicle Propulsion Systems: Introduction to Modeling and Optimization*. Springer, 2005.

**26.** Willis, R. *Principles of Mechanism, Second Edition*. Longmans, Green and Co., 1870.

**27.** Sciaretta A. and Guzzella, L. "Control of Hybrid Electric Vehicles," *Control Systems, IEEE*, vol. 27, no. 2, pp. 60-70, 2007.

**28.** Marano, V., Tulpule, P., Stockar, S., Onori, S. et al., "Comparative study of Different Control Strategies for Plug-In Hybrid Electric Vehicles," SAE Technical Paper 2009-24-0071, 2009, doi: 10.4271/2009-24-0071.

**29.** Stockar, S. Marano, V. Canova, M. Rizzoni, G. and Guzzella, L. "Energy-optimal control of plug-in hybrid electric vehicles for real-world driving cycles," *Vehicular Technology, IEEE Transactions on*, vol. 60, pp. 2940-2962, 2011.

**30.** Serrao, L. Onori, S. and Rizzoni, G. "ECMS as a realization of Pontryagin's Minimum Principle for HEV control," in *Proceedings of the American Control Conference*, 2009.

**31.** Kim N. and Rousseau, A. "Sufficienct conditions of optimal control based on pontryagin's minimum principle for use in hybrid electric vehicles," *IMechE Part D: J. of Automobile Engineering*, 2012.

**32.** Zhang C. and Vahidi, A. "Route preview in energy management of plug-in hybrid vehicles," *Control Systems Technology, IEEE Transactions on*, vol. 20, no. 2, pp. 546-553, March 2012.

**33.** Ciccarese, G. Donateo, T. Marra, P. Pacella, D. and Palazzo, C. "Vehicular communications for efficient energy management of hybrid electric vehicles," *FISITA 2010*, May 30-June 4, 2010.